Electrochemical Model-Based Condition Monitoring via Experimentally Identified Li-Ion Battery Model and HPPC †

Md Ashiqur Rahman [1], Sohel Anwar [1],* (ID) **and Afshin Izadian [2]**

[1] Department of Mechanical Engineering, Indiana University–Purdue University Indianapolis, Indianapolis, IN 46202, USA; ashique027@gmail.com

[2] Energy Systems and Power Electronics Laboratory, Indiana University–Purdue University Indianapolis, Indianapolis, IN 46202, USA; aizadian@iupui.edu

* Correspondence: soanwar@iupui.edu; Tel.: +1-317-274-7640

† This paper is an extended version of our paper published in Rahman, M.A.; Anwar, S.; Izadian, A. Electrochemical model based fault diagnosis of a lithium ion battery using multiple model adaptive estimation approach. In Proceedings of the 2015 IEEE International Conference on Industrial Technology (ICIT), Seville, Spain, 17–19 March 2015.

Abstract: Electrochemical model-based condition monitoring of a Li-Ion battery using an experimentally identified battery model and Hybrid Pulse Power Characterization (HPPC) cycle is presented in this paper. $LiCoO_2$ cathode chemistry was chosen in this work due to its higher energy storage capabilities. Battery electrochemical model parameters are subject to change under severe or abusive operating conditions resulting in, for example, Navy over-discharged battery, 24 h over-discharged battery, and overcharged battery. Stated battery fault conditions can cause significant variations in a number of electrochemical battery model parameters from nominal values, and can be considered as separate models. Output error injection based partial differential algebraic equation (PDAE) observers have been used to generate the residual voltage signals in order to identify these abusive conditions. These residuals are then used in a Multiple Model Adaptive Estimation (MMAE) algorithm to detect the ongoing fault conditions of the battery. HPPC cycle simulated load profile based analysis shows that the proposed algorithm can detect and identify the stated fault conditions accurately using measured input current and terminal output voltage. The proposed model-based fault diagnosis can potentially improve the condition monitoring performance of a battery management system.

Keywords: electrochemical model; lithium-ion batteries; fault diagnosis; MMAE; PDAE observer; battery management system

1. Introduction

Lithium ion battery is deemed as one of the most promising sources of alternative energy storage devices for numerous applications, like hybrid electric, plug-in hybrid electric and electric vehicles, as well as major portable electronic devices [1]. Moreover, compared to the other alternative options for energy, Li-Ion batteries have some unique advantages including: these batteries have minimum memory effect, have higher specific energy, provide the best energy-to-weight ratio, and have low self-discharge when idle [2,3]. Based on these stated advantages, Li-ion batteries are the leading candidate for the upcoming generation of aerospace, automotive, and other applications.

Electric Vehicles (EV), Plug-in Hybrid Electric Vehicles (PHEV), and Hybrid Electric Vehicles (HEV) have been gaining more acceptance in recent years due to their low emissions and better

fuel efficiencies [4]. Performance of these transportation options is significantly dependent on the electrochemical energy sources, e.g., installed battery modules integrated with generic transmission system. Installed batteries undergo different operating conditions depending on the user driving habits and the road conditions as the battery load demand changes due to the stated factors. Undoubtedly, a safe operation of the entire battery module is always expected, as it is one of the most vital components of the vehicle's configurations. However, it is not always possible to maintain the desired safe and healthy operating conditions of the battery system for a number of reasons. For instance, a Li-Ion battery can be overcharged or over-discharged during operation at different rates based on the vehicle's operating conditions (e.g., sudden power demand leading to over-discharge of battery, sudden rush of power to charge battery in regenerative braking). In addition to the stated operating conditions, aging due to the long term cycling of the battery is another potential contributor to battery electrochemical model parameter changes.

The onboard battery management system is responsible for managing the rechargeable battery system by monitoring its state of operation, protecting the battery from unsafe operating zones, and reporting the diagnostic data to the operator while managing the battery operation. Monitoring of different battery fault conditions is crucial to ensure the optimal operation of Li-Ion battery without negatively impacting the safety or expected battery life.

All of the model based fault detection and diagnosis (FDD) techniques make use of two major types of model, namely the equivalent circuit-based models and true physics-based models. In equivalent circuit-based models, the battery is modeled by assuming that the true behavior of the battery is attainable by using a combination of resistors, capacitors, voltage sources, and Warburg impedances. This approach does not deal with the real dynamics of the battery chemistry.

On the other hand, the real physics-based models, such as the one presented by Doyle, Fuller, and Newman [5] are primarily based on partial differential equations, which capture the kinetics of the battery chemistry more realistically. This electrochemical model is based on the concentrated solution theory [6]. Model reduction via realistic simplifying assumption is used in this work, as this model is too complex to be used in a real time application. The work presented here is based on the reduced order partial differential equation [1], representing the electrochemical battery model.

A large body of work exists that aims at the fault detection and diagnosis of rechargeable batteries. Among them, adaptive estimation technique has been used in [7], which is based on the equivalent circuit model. The Extended Kalman Filter (EKF) used in this work is based on a polynomial approximation of the nonlinearity in the model. An adaptive recurrent neural network (ARNN) was used for the prediction of remaining useful life (RUL) in [8], which also used equivalent circuit models. Synthesized design of Luenberger observer (LO) was adopted in [9], which used equivalent circuit model for fault isolation and estimation.

In [10], a data-driven method is presented on the diagnosis and prognosis of the battery health in an alternative powertrain. The authors used a support vector machine (SVM) type machine learning technique for estimation purposes. A similar methodology using a conditional three-parameter capacity degradation model was presented in [11]. Kozlowski [12] presented a battery parameter identification, estimation, and prognosis methodology using a number of methodology, e.g., neural network (NN), auto regressive moving average (ARMA), fuzzy logic (FL), and impedance spectroscopy (IS), etc. Since the data-driven methods are based on the input-output relationship without any insight into the process, the real physics of the battery model is ignored in such approaches.

A sliding mode observer is utilized for fault diagnosis purposes in [13], whereas a partial differential algebraic equation (PDAE) based observer is incorporated for fault detection in [14]. In sliding mode control (SMC), the non-linearity of the battery dynamics is leveraged by applying discontinuous control signal in order to generate the desired output for the system under consideration. The use of PDAE observer, on the other hand, takes advantage of the physics based non-linear model of Li-Ion battery to improve the accuracy of fault detection.

Electrochemical model based multiple model adaptive estimation has been introduced to detect the ongoing fault(s) in a lithium ion battery in [15]. This adaptive estimation method requires representation of different fault scenarios, generation of the residual signals, and then the isolation of the different types of faults using the proposed algorithm. The generation and evaluation of residuals plays a vital role on the performance of fault diagnosis. However, model parameters used in this work were borrowed from existing literature, which may not be representative of the battery chemistry and conditions considered here. Urban Dynamometer Driving Schedule (UDDS) has been used to validate the proposed algorithms. However, a Hybrid Pulsed Power Characterization (HPPC) is more appropriate for batteries used in hybrid and electric vehicles for design purposes [16].

In this work, experimentally identified electrochemical models have been used to detect fault conditions in a lithium ion battery using multiple model adaptive estimation method. Here the residuals are generated by comparing the simulated outputs of the fault models with the simulated output of the true plant model. A number of electrochemical model parameters (for each of the fault conditions) were identified using a gradient free particle swarm optimization algorithm [17] on a reduced order model of lithium ion battery. An EKF based estimation method has been considered in [18], where internal electrochemical variables were estimated by using the reduced order model of a Li-Ion battery derived from a 1D physics based model.

Work presented here aims at detecting several fault conditions, namely, Navy over-discharge (OD), 24 h OD, and over-charge (OC) conditions, along with the detection of a healthy battery [7]. Among the stated fault scenarios in a Li-ion battery, OD and OC are critical for maintaining the health of the battery. While over-charging can cause overheating that can lead to the vaporization of the active material and possibly explosion, over-discharge can short circuit the battery cell [19–23]. However, if these faults can be detected quickly according to the described methodology, steps can be taken to solve the issues before the faults can deteriorate to their extreme conditions. In this work, multiple model adaptive estimation (MMAE) algorithm has been used in the detection of the stated battery operating conditions, i.e., fault diagnosis of the battery for an input load current from the hybrid pulse power characterization (HPPC) cycle simulated on a hybrid vehicle.

Sections 2 and 3 of this paper illustrate a reduced electrochemical battery model and the corresponding PDAE observer. Section 4 presents the experimentally identified electrochemical model parameters for various fault conditions from earlier work. Section 5 briefly describes the multiple model adaptive estimation method adopted in this work. Section 6 presents the validation results of battery fault diagnosis using the HPPC cycle. Finally, the findings are summarized in the conclusion section.

2. Reduced Electrochemical Battery Model

A reduced electrochemical model of lithium ion battery was presented in [15] based on a few simplifying assumptions. The reduced model allowed for the simulation of the cell dynamics while maintaining the accuracy. The key assumption made here is that the electrolyte concentration is constant. An approximate solution of the diffusion equations in the solid active materials in each electrode has been used as presented in [24,25]. Figure 1 illustrates a schematic of the Li-Ion battery electrochemical model. Using these two assumptions, the reduced order PDAE equations can be presented as follows [15]:

$$\frac{\partial}{\partial t}\bar{c}_{s,i}{}^{\pm}(x,t) = -\frac{3}{R_i{}^{\pm}}j_{n,i}{}^{\pm}(x,t) \tag{1}$$

$$\frac{\partial}{\partial t}\bar{q}_{s,i}{}^{\pm}(x,t) = -\frac{30}{(R_i{}^{\pm})^2}\bar{q}_{s,i}{}^{\pm}(x,t) - \frac{45}{2(R_i{}^{\pm})^2}j_{n,i}{}^{\pm}(x,t) \tag{2}$$

$$c_{ss,i}{}^{\pm}(x,t) = \bar{c}_{s,i}{}^{\pm}(x,t) + \frac{8R_i{}^{\pm}}{35}\bar{q}_{s,i}{}^{\pm}(x,t) - \frac{R_i{}^{\pm}}{35D_{s,i}{}^{\pm}}j_{n,i}{}^{\pm}(x,t) \tag{3}$$

$$j_{n,i}^{\pm}(x,t) = \frac{i_{0,i}^{\pm}(x,t)}{F}\left(e^{\frac{\alpha_a F \eta_i^{\pm}(x,t)}{RT}} - e^{\frac{-\alpha_C F \eta_i^{\pm}(x,t)}{RT}}\right) \tag{4}$$

$$\frac{\partial i_e^{\pm}(x,t)}{\partial x} = \sum_{i=1}^{i=n}\frac{3\varepsilon_{s,i}^{\pm}}{R_{p,i}^{\pm}}Fj_{n,i}^{\pm}(x,t) \tag{5}$$

$$\frac{\partial \varphi_s^{\pm}(x,t)}{\partial x} = \frac{i_e^{\pm}(x,t) - I(t)}{\sigma^{\pm}} \tag{6}$$

$$\frac{\partial \varphi_e^{\pm}(x,t)}{\partial x} = -\frac{i_e^{\pm}(x,t)}{\kappa} \tag{7}$$

$$\rho^{avg}c_p\frac{dT(t)}{dt} = h_{cell}(T_{amb} - T(t)) + I(t)V(t) - \sum_{i=1}^{i=n}\left[\int_{0^-}^{L^-}\frac{3\varepsilon_{s,i}^-}{R_{p,i}^-}Fj_{n,i}^-(x,t)\Delta U_i^-(x,t)dx\right]$$
$$- \sum_{i=1}^{i=n}\left[\int_{0^+}^{L^+}\frac{3\varepsilon_{s,i}^+}{R_{p,i}^+}Fj_{n,i}^+(x,t)\Delta U_i^+(x,t)dx\right] \tag{8}$$

Boundary conditions for the above reduced order model are given by:

$$\varphi_e^+(0^+,t) = 0, i_e^{\pm}(0^{\pm},t) = 0$$

$$\varphi_e^-(L^-,t) = \varphi_e^+(L^+,t) - \frac{I(t)L^{sep}}{\kappa^{sep}}; \text{ and } i_e^{\pm}(L^{\pm},t) = \pm I(t)$$

The initial conditions of this model are:

$$c_{s,i}^{\pm}(x,0) = \bar{c}_{s,i,0}^{\pm}(x), \bar{q}_{s,i}^{\pm}(x,0) = \bar{q}_{s,i,0}^{\pm}(x), T(0) = T_0$$

The output equation for this reduced order model remains the same as previously mentioned, i.e.,

$$V(t) = \varphi_s(0^+,t) - \varphi_s(0^-,t) \tag{9}$$
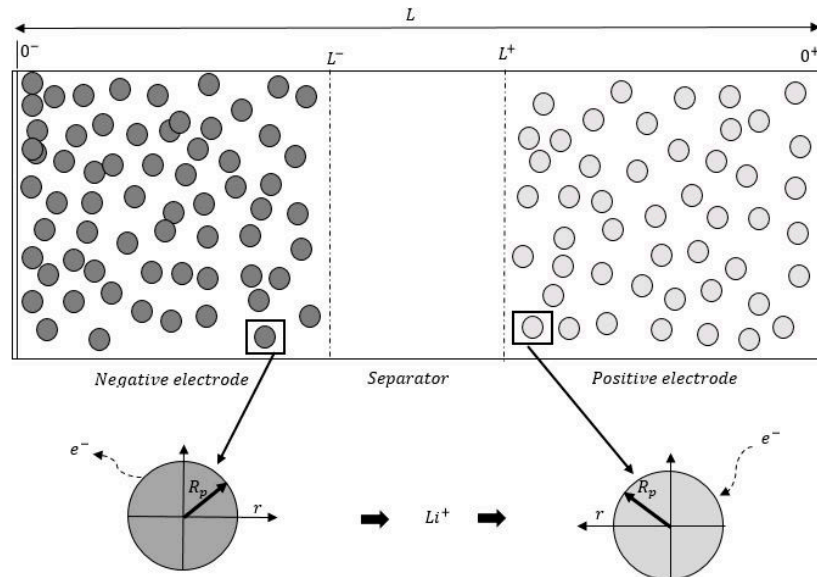

Figure 1. Schematic of Li-Ion battery electrochemical model.

3. PDAE Observer

The PDAE observer equations use an error between the measured and calculated voltages as feedback. This error feedback is maintained in such a way that all of the variables being estimated

converge to their true values [21]. The PDAE observer equations are written for the volume averaged concentrations in the individual electrodes as follows:

$$\frac{\partial}{\partial t}\overline{\hat{c}_{s,i}}^{\pm}(x,t) = -\frac{3}{R_i^{\pm}}\overline{\hat{j}_{n,i}}^{\pm}(x,t) + \gamma_i^{\pm}(V(t) - \hat{V}(t)) \tag{10}$$

The above observer uses Equations (2)–(8) as a part of the observer model. The output equation of the observer is:

$$\hat{V}(t) = \hat{\phi}_s(0^+, t) - \hat{\phi}_s(0^-, t) \tag{11}$$

The equations of the observer gain in the two electrodes are given by [1]:

$$\begin{bmatrix} \gamma_i^- \\ \gamma_i^+ \end{bmatrix} = \begin{bmatrix} \frac{1}{n_a^- \varepsilon_{s,i}^- L^-} \\ \frac{1}{n_a^+ \varepsilon_{s,i}^+ L^+} \end{bmatrix} \tag{12}$$

where, n_a denotes number of active materials which is assumed as one in this work. The battery temperature is assumed to be constant at room temperature, i.e., 298.15 K. This assumption is based on the fact that all the batteries were tested at room temperature in this work.

4. Identified Electrochemical Model Parameters

Among all of the electrochemical model parameters of the battery dynamics, some parameters are dependent on the battery physics, while other parameters depend on the electro-chemistry of the battery [25]. A number of these parameters are adopted from the manufacturer provided values.

A majority of the battery parameters were unchanged under the abusive operating conditions, such as overcharging and over-discharging. These parameter values were adopted from [26]. However, four important battery parameters (e.g., diffusion coefficients or diffusivity in both positive and negative electrodes and intercalation/de-intercalation reaction rates at both positive and negative electrodes) were found to change appreciably under these abusive operating conditions. These four parameters were experimentally identified in [17]. These experimentally identified parameters offered a higher degree of reliability of the electrochemical battery model and hence used in this work. These parameters are initialized with the values provided in Table 1 [17,27]:

Table 1. Initial values of the parameters to be identified.

Parameter to Identify	Initial Maximum Value
$D_{s,p}$	1×10^{-15}
$D_{s,n}$	2×10^{-16}
K_p	3×10^{-14}
K_n	5×10^{-16}

The objective function/fitness function used for the parameter identification method via particle swarm optimization (PSO) algorithm is given by the following function [17,28]:

$$\min \int_{t=1}^{t=n} (V_e - V_m)^2 \, dt \tag{13}$$

Here, V_m is the model predicated voltage corresponding to an input current signal, V_e is measured experimental voltage corresponding to the same input current, t is the number of samples in the current signal and n is the number of iterations in PSO algorithm [17,29].

In [17], the authors provided four different operating conditions of the battery, i.e., healthy, Navy over-discharge, 24 h over-discharge, and over-charge conditions. The parameters were identified for

both charging and discharging operation of battery, which provides more robustness to the battery models. The identified parameters for different operating conditions are provided in Tables 2–5 [17]:

Table 2. Identified items for healthy battery.

Identified Item	For Discharge	For Charge
$D_{s,p}$	4.0264×10^{-16}	1.7507×10^{-15}
$D_{s,n}$	4.3196×10^{-14}	4.6174×10^{-15}
K_p	6.0555×10^{-14}	7.7358×10^{-14}
K_n	3.5484×10^{-15}	1.0532×10^{-14}

Table 3. Identified items for Navy-over-discharge (OD) battery.

Identified Item	For Discharge	For Charge
$D_{s,p}$	6.5418×10^{-16}	2.0828×10^{-15}
$D_{s,n}$	3.35×10^{-15}	9.3458×10^{-16}
K_p	7.3194×10^{-13}	5.4301×10^{-14}
K_n	1.1129×10^{-15}	8.4599×10^{-15}

Table 4. Identified items for 24 h OD battery.

Identified Item	For Discharge	For Charge
$D_{s,p}$	4.0995×10^{-16}	1.8848×10^{-15}
$D_{s,n}$	3.6899×10^{-15}	9.5869×10^{-15}
K_p	2.1611×10^{-13}	5.0345×10^{-14}
K_n	1.0775×10^{-15}	3.3563×10^{-15}

Table 5. Identified items for over-charge (OC) battery.

Identified Item	For Discharge	For Charge
$D_{s,p}$	1.2884×10^{-16}	2.0986×10^{-15}
$D_{s,n}$	9.7622×10^{-15}	1.9827×10^{-14}
K_p	3.3685×10^{-13}	3.3064×10^{-14}
K_n	1.9175×10^{-15}	2.4734×10^{-15}

In this work, parameters were used conditionally, meaning that parameters for the charging region of the battery operation were used in case of over-charged battery. For the Navy-OD and 24 h OD battery, discharge region identified parameters were used. For healthy battery model, discharge region parameters were used in case of healthy battery discharge [17,27].

5. Multiple Model Adaptive Estimation Based Fault Identification

This adaptive estimation technique is used to detect and identify battery fault conditions using the electrochemical model of Li-ion battery in this work. In this estimation (MMAE) technique [7,30–36], as illustrated in Figure 2, various models run simultaneously while all of the models are excited by a same input signal. MMAE in this work uses PDAE observer outputs of different models (arising out of parameter variations) to generate residuals. If there are a total of "n" models, there can be $(n - 1)$ outputs representing the faults or unhealthy scenarios [7,30]; the remaining one is the actual plant model output.
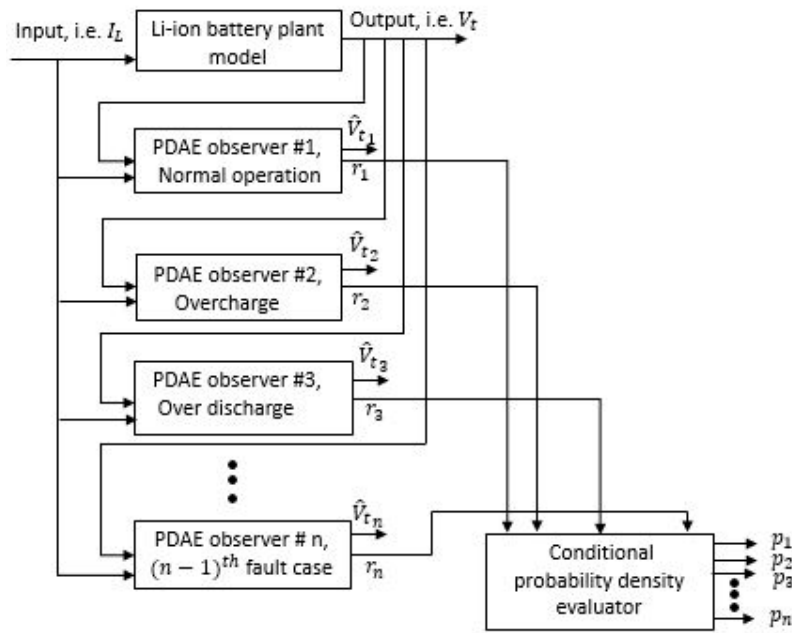
Figure 2. Multiple model adaptive estimation (MMAE) algorithm skeleton.

One of the distinguishing features of MMAE method is that it provides a scope of fault detection based on possible fault scenarios along with the actual model. The principal advantage of MMAE as compared with other possible ways of fault detection (fuzzy logic, SVM etc.) is that it provides a probabilistic approach to condition monitoring [7,36] based on the differences of outputs between the actual model and all other individual fault models, which is considered more reliable in fault diagnosis.

The summation of all conditional probabilities of the concerned models in Figure 2 must be unity, i.e.,

$$p_1 + p_2 + p_3 + \ldots \ldots + p_n = 1 \tag{14}$$

The conditional probabilities require a priori samples to compute the current values and are normalized over a complete sum of conditional probabilities of all systems. The probability for the *n*-th model at time sample *k* is given by [7,31,33,35]:

$$p_{n,k} = \frac{f_{z(k)|a,z(k-1)}\left(z_k \middle| a_n, z_{k-1}\right) p_n(k-1)}{\sum\limits_{j=1}^{j=n} f_{z(k)|a,z(k-1)}\left(z_k \middle| a_j, z_{k-1}\right) p_j(k-1)} \tag{15}$$

where $f_{z(k)|a,z(k-1)}\left(z_k \middle| a_n, z_{k-1}\right) p_n(k-1)$ is the conditional probability density function of the model considering the history of all measurements.

The conditional probability function is expressed as [31,33,35]:

$$f_{z(k)|a,z(k-1)}\left(z_k \middle| a_n, z_{k-1}\right) p_n(k-1) = \beta_n \exp(\circ)$$

$$\beta_n = \frac{1}{(2\Pi)^{L/2} |\psi_n(k)|^{1/2}}; (\circ) = \frac{1}{2} r_{n,k}{}^T \psi_{n,k}{}^{-1} r_{n,k}$$

L is the measurement dimension and equal to 1.

$r_{n,k} = V_{m_{n,k}} - V_{o_{n,k}}$ is the residual signal for the *n*-th model at time sample *k* .

$V_{m_{n,k}}$ is associated measured voltage; $V_{o_{n,k}}$ is associated observer voltage.

When the output of any of the available models matches with the output of the actual model, which simultaneously drives the mean value of that residual signal to zero, the covariance of that particular signal is given by [31,33,35]:

$$\psi_{n,k} = C_{n,k} P_{n,k|k} C_{n,k}{}^T + R \tag{16}$$

where $C_{n,k}$ is the output vector for *n*-th system at any time sample *k*. Moreover, $P_{n,k|k}$ represents the state covariance matrix while R is covariance matrix of measurement noise.

Using all possible residuals, the conditional probabilities are evaluated. The largest conditional probability may be used as an indication of ongoing fault condition based on that particular specific residual [7,36].

6. Validation of Fault Diagnosis Algorithm via Hybrid Pulse Power Characterization (HPPC) Cycle

Multiple model adaptive estimation (MMAE) technique was implemented for a general sinusoidal battery input current profile successfully in [35]. Additionally, four critical battery parameters were identified experimentally [17], as mentioned in parameter identification section. These different sets of identified parameter groups formed the model bank for the abusive battery conditions as well as the healthy battery, which are to be used in the MMAE fault diagnosis algorithm. The identified battery models will now be applied to the adaptive estimation algorithm in order to obtain a more realistic and accurate fault diagnosis of the battery abusive conditions. As mentioned earlier, four operating conditions of the battery will be used in the fault diagnosis, i.e., Healthy battery, Navy over discharged battery, 24 h over discharged battery, and over-charged battery.

Batteries were tested using CADEX C8000 battery tester. The battery states under consideration were obtained via experimentations using the following charge/discharge regimes:

1. Healthy battery charge-discharge regime: The Li-Ion battery is discharged at a nominal rate of 1C to a low state of charge (SOC) (below 10%). This is followed by a nominal (1C) charging of the battery to a fully charged state. This cycle is repeated 20 times and the critical battery parameters are monitored.
2. Navy over-discharged cycle: The Li-ion battery is discharged at maximum suitable discharge rate of 25% over discharge (1.25C). The charging of the battery is carried out using a standard non-abusive charge regime (1C). The battery is cycled 20 times using this discharge-charge regime and the critical battery parameters are monitored.
3. 24 h over-discharged cycle: The Li-Ion battery is discharged at a suitable discharge rate (1.2C) until the SOC reaches zero. To maintain near zero terminal voltage, a resistor is connected across the terminals for the duration of 24 h. The charging of the battery is then carried out using a standard non-abusive charging profile (1C). The 24 h over discharge test cycle is repeated 20 times and the battery parameters are monitored.
4. Overcharged battery cycle: The Li-Ion battery is discharged at a nominal discharge rate (1C) to a low SOC level (below 10%). This is followed by a 25% over-charge (1.25C) of the battery. This cycles is repeated 20 times and the critical battery parameters are monitored.

For the fault diagnosis purposes, the experimentally identified battery models obtained through the above tests were simulated for an input load current based on hybrid pulse power characterization (HPPC) cycle vehicle operation [37]. Hybrid pulse power characterization is vital in EV, PHEV, or HEV because of its' applicability in determining the dynamic power capability over the usable charge and voltage range of the concerned vehicle, or the device where both discharge and regenerative pulses are considered in the test profile current signal [37]. Therefore, fault diagnosis based on the battery current output from a HPPC cycle simulation of a HEV can be an important step in the fault diagnosis of Li-Ion battery.

The battery load profile (HPPC cycle simulated) used in the fault diagnosis is shown in Figure 3. This represents a portion of the HPPC cycle simulated output current profile, which has been used for all battery models considered in this work. In details, both plant and observer models were simulated for this same input current profile, and the difference output yielded the residuals, which were used in conditional probability observations.
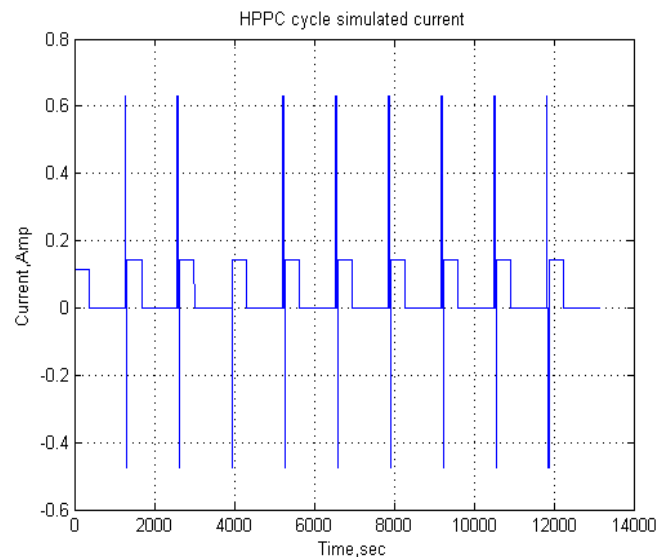

Figure 3. Hybrid Pulse Power Characterization (HPPC) cycle simulated load profile used in fault diagnosis.

All four models were simulated for this load current profile generating the battery response voltages. Moreover, the PDAE observer model was also run for each of the battery operating conditions to generate the residuals for the fault diagnosis purpose.

The response from the experimentally identified model and that of the PDAE observer against the HPPC load profile input for the healthy battery operation are provided in Figure 4.
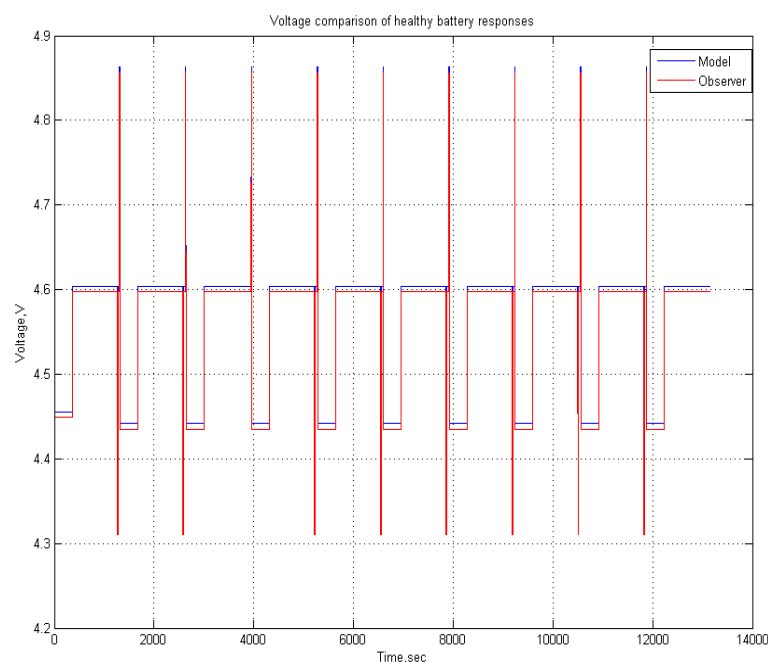

Figure 4. Model and observer response differences for healthy operating of battery.

Similarly, for Navy over discharged battery operation, the experimentally identified model and observer voltage response comparison for the HPPC load profile input is provided in Figure 5.
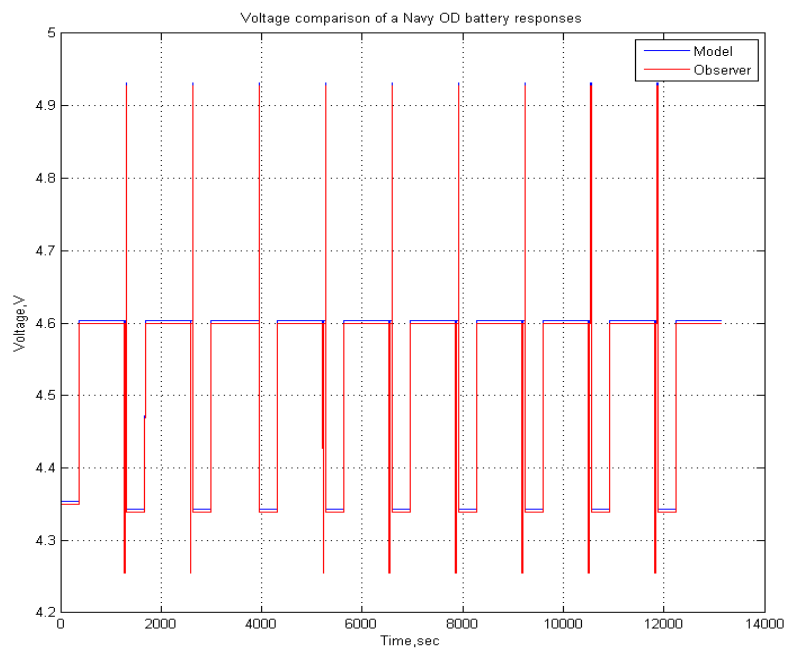

Figure 5. Model and observer response differences for Navy OD battery operation.

Observed voltage is compared with the experimentally identified model simulated voltage for in response to an HPPC load profile input for the 24 h over discharged battery is provided in Figure 6.
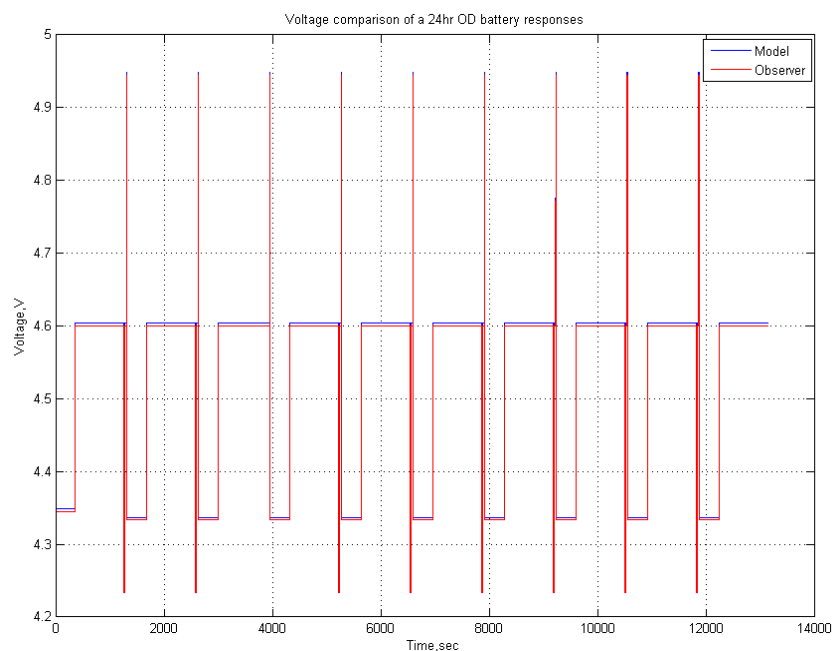

Figure 6. Model and observer response differences for 24 h OD battery operation.

Similar comparison of the response voltages against the HPPC load profile input for over charged battery operation is illustrated in Figure 7.
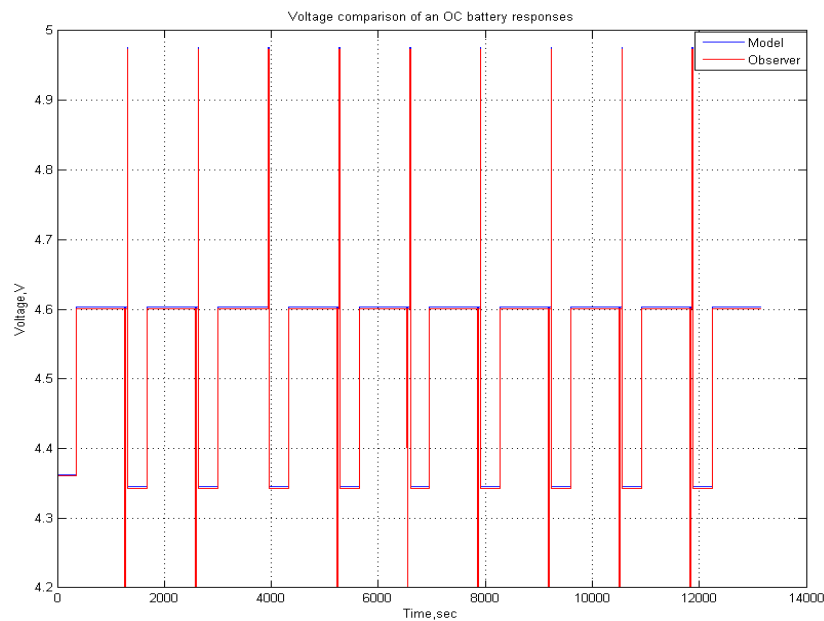
Figure 7. Model and observer response differences for OC battery operation.

As mentioned earlier, the output battery voltages of the experimentally identified models and observer battery models were recorded for the same HPPC load profile input current. Figures 4–7 show the differences between the responses of the two stated models (i.e., experimentally identified model and observer model) for different battery operating conditions. Clearly, the difference in battery output voltage is too small to notice in all four cases. This is due to the superior accuracy in the observer model response, where observer followed the plant model closely.

For the fault diagnosis purpose, a plant model voltage profile was defined to induce the stated fault conditions with an aim to generate the residuals to be used in MMAE algorithm. For this plant model voltage profile generation, following described procedure was adopted:

1. the total duration for the HPPC cycle simulated load current profile was 13,140 s;
2. within this total length of fault diagnosis time, the first 2628 s were allocated for Healthy battery model;
3. the following 1314 s were allocated for the Navy OD battery model;
4. the following 2628 s were allocated for 24 h OD battery, followed by 1314 s of Healthy battery operation; and,
5. the following 2628 s were allocated for OC battery, and the last 2628 s were again allocated for Healthy operation of the battery.

Following the above sequence of battery operation, the resulting battery output voltage profile is generated, as shown in Figure 8.

As mentioned previously, PDAE observer responses for all of the battery operating conditions are subtracted from the plant voltage responses, and the residuals are generated for particular battery model. The voltage residuals are provided in Figure 9.
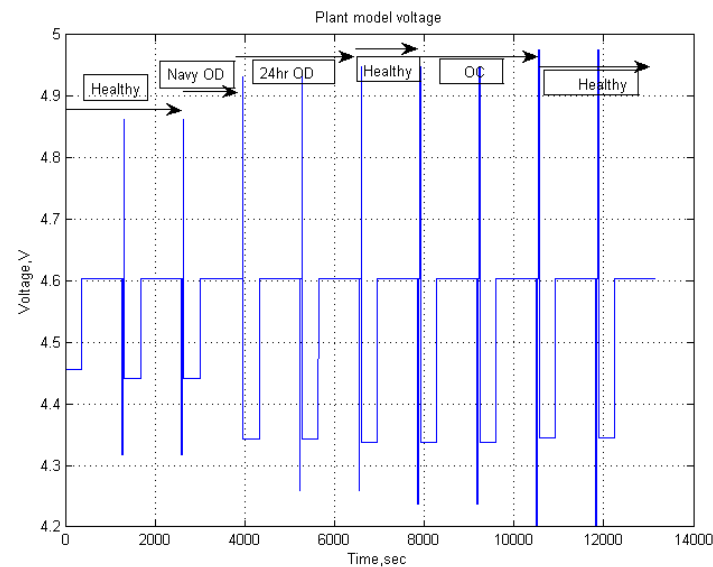
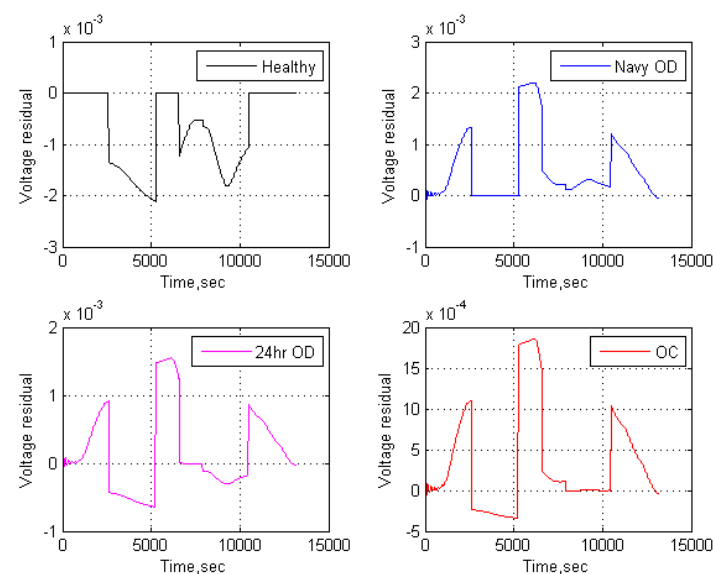**Figure 8.** Considered plant model voltage profile.

Figure 9. Calculated voltage residuals of respective battery models.

For different operating conditions of the battery, the state covariance matrices are obtained by using the system identification methodology. Using these state covariance matrices and the voltage residuals, the conditional probability densities are generated for different values of measurement noise covariance matrix, *R*. If the voltage residual presented in this fault diagnosis scheme is analyzed, it is clear that the maximum value of system residual or the noise signal is in the range of 10^{-4}. Therefore, the measurement noise covariance matrix should be lower than the maximum system noise signal. Conditional probabilities were obtained using different values of measurement covariance matrices, which is obviously lower than the maximum system noise.

For example, if $R = 1 \times 10^{-5}$, the resultant conditional probabilities for different operating conditions provided by the MMAE algorithm are shown in Figure 10.
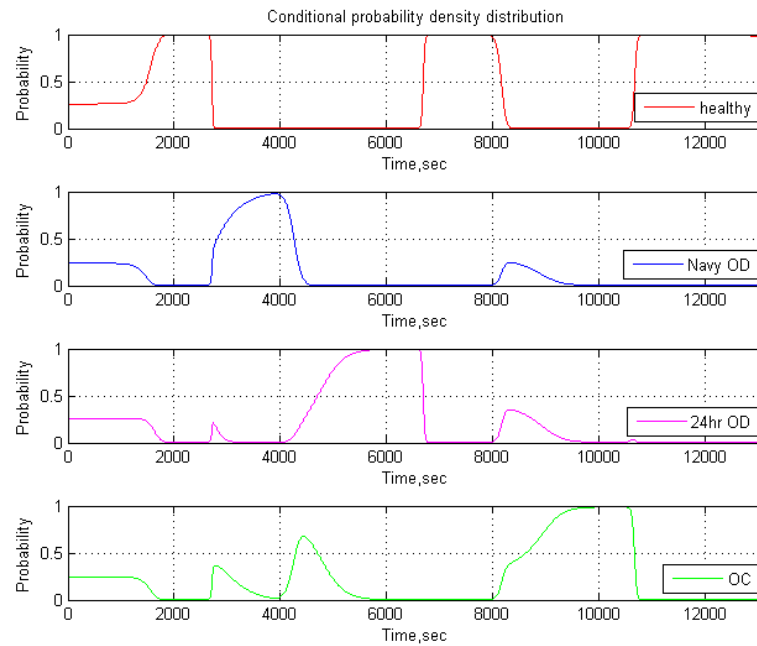
Figure 10. Conditional probability densities of respective battery operating conditions for $R = 1 \times 10^{-5}$.

For $R = 1 \times 10^{-8}$, the conditional probability distribution provided by the MMAE algorithm are shown in Figure 11.
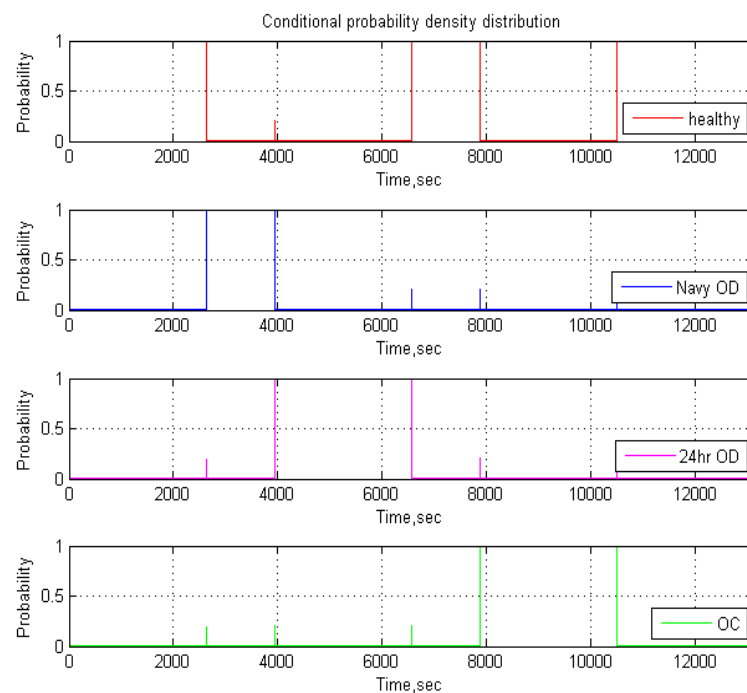

Figure 11. Conditional probability densities of respective battery operating conditions for $R = 1 \times 10^{-8}$.

If the detected probability of the operating conditions is observed, it is clear that the fault diagnosis is not accurate for the given set of the values taken in MMAE algorithm. It was observed that the measurement covariance matrix has a significant contribution in the fault diagnosis accuracy. To have a better fault diagnosis, MMAE algorithm was tuned to have the better identification of the operating conditions.

Observing this probability distribution, it is clear that the fault scenarios of battery operations that were created were perfectly detected. Since the considered models were identified experimentally by PSO algorithm for the battery sets, the detection of operating conditions or this fault diagnosis for these tested battery sets offers a more reliable and realistic condition monitoring, which can be integrated into the battery management system for improved overall performance.

7. Conclusions

In this paper, experimentally identified electrochemical battery model parameters for different abusive operating conditions of a Li-Ion battery in prior studies were adopted for the fault diagnosis purpose. Multiple model adaptive estimation algorithms were implemented for detecting the stated fault conditions of the battery. Since the battery model parameters were experimentally identified a priori for each of these abusive conditions, detection of these fault conditions using the realistic HPPC cycle simulated load current profile provided a robust basis for fault diagnosis. Each of these identified models was matched accurately with the injected fault conditions through the MMAE algorithm, which yielded a reliable method for condition monitoring. Battery temperature variation was assumed as constant and this constant temperature assumption was verified while experiments were carried out. However, multi-dimensional battery model analysis can be taken as a future research work to further improve the 1-D model based FDD algorithm, as presented in this work. Additionally, the proposed diagnostic methodology can thus enhance the accuracy of fault detection for a battery management system for Li-Ion batteries.

Author Contributions: M.A.R. and S.A. conceived and designed the experiments; A.I. provided information on MMAE algorithm; M.A.R. performed the experiments; M.A.R., A.I. and S.A. analyzed the data; M.A.R. wrote the paper.

Conflicts of Interest: The authors declare no conflicts of interest.

Nomenclature

c_e	Lithium ion concentration in the electrolyte phase
c_s	Lithium ion concentration in the active materials in both electrodes
$\bar{c}_{s,i}$	Volume-averaged concentration of a single particle
D_e	Diffusivity at electrolyte phase
D_s	Diffusivity at solid phase
$f_{\frac{c}{a}}$	Mean molar activity coefficient
F	Faraday constant
i_e	Current in the electrolyte phase
i_0	Exchange current density
I	Load current
j_n	Molar ion fluxes between the active materials in electrodes and the electrolyte
L^-	Length of negative electrode
L^+	Length of positive electrode
n	Number of active materials
R	Universal gas constant
R_p	Radius of the spherical particles
t_c^0	Transference number
T	Average internal temperature
U	Open circuit potential

V	Cell voltage
α_a	Charge transfer coefficient in anode
α_c	Charge transfer coefficient in cathode
γ	Observer gain constant
φ_e	Potential at electrolyte phase
φ_s	Potential at solid phase
ε_e	Volume fraction at electrolyte phase
ε_s	Volume fraction at solid phase
η	Over-potential for the reactions
ρ^{avg}	Average density
κ	Rate constant for the electrochemical reaction

References

1.　Klein, R.; Chaturvedi, N.A.; Christensen, J.; Ahmed, J.; Findeisen, R.; Kojic, A. Electrochemical model based observer design for a lithium-ion battery. *IEEE Trans. Control Syst. Technol.* **2013**, *21*, 289–301. [CrossRef]

2.　Tarascon, J.M.; Armand, M. Issues and challenges facing rechargeable lithium batteries. *Nature* **2001**, *414*, 359–367. [CrossRef] [PubMed]

3.　Chaturvedi, N.A.; Klein, R.; Christensen, J.; Ahmed, J.; Kojic, A. Modeling, estimation, and control challenges for lithium-ion batteries. In Proceedings of the American Control Conference (ACC), Baltimore, MD, USA, 30 June–2 July 2010.

4.　Wouk, V. Hybrid electric vehicles. *Sci. Am.* **1997**, *277*, 70–74. [CrossRef]

5.　Doyle, M.; Fuller, T.F.; Newman, J. Modeling of galvanostatic charge and discharge of the lithium/polymer/insertion cell. *J. Electrochem. Soc.* **1993**, *140*, 1526–1533. [CrossRef]

6.　Newman, J.; Tiedemann, W. Porous-electrode theory with battery applications. *AIChE J.* **1975**, *21*, 25–41. [CrossRef]

7.　Sidhu, A.; Izadian, A.; Anwar, S. Model Based Condition Monitoring in Lithium-Ion Batteries. *J. Power Sources* **2014**, *268*, 459–468.

8.　Liu, J.; Saxena, A.; Goebel, K.; Saha, B.; Wang, W. An adaptive recurrent neural network for remaining useful life prediction of lithium-ion batteries. In Proceedings of the 2010 Annual Conference of the Prognostics and Health Management Society (PHM), Portland, OR, USA, 10–14 October 2010.

9.　Chen, W.; Chen, W.; Saif, M.; Li, M.; Wu, H. Simultaneous fault isolation and estimation of Lithium-Ion batteries via synthesized design of Luenberger and learning observers. *IEEE Trans. Control Syst. Technol.* **2014**, *1*, 290–298. [CrossRef]

10.　Nuhic, A.; Terzimehic, T.; Soczka-Guth, T.; Buchholz, M.; Dietmayer, K. Health diagnosis and remaining useful life prognostics of lithium-ion batteries using data-driven methods. *J. Power Sources* **2013**, *239*, 680–688. [CrossRef]

11.　Wang, D.; Miao, Q.; Pecht, M. Prognostics of lithium-ion batteries based on relevance vectors and a conditional three-parameter capacity degradation model. *J. Power Sources* **2013**, *239*, 253–264. [CrossRef]

12.　Kozlowski, J.D. Electrochemical cell prognostics using online impedance measurements and model-based data fusion techniques. In Proceedings of the Aerospace Conference, Big Sky, MT, USA, 8–15 March 2003.

13.　Dey, S.; Ayalew, B. A Diagnostic Scheme for Detection, Isolation and Estimation of Electrochemical Faults in Lithium-ion Cells. In Proceedings of the ASME 2015 Dynamic Systems and Control Conference, Columbus, OH, USA, 28–30 October 2015.

14.　Marcicki, J.; Onori, S.; Rizzoni, G. Nonlinear fault detection and isolation for a lithium-ion battery management system. In Proceedings of the ASME 2010 Dynamic Systems and Control Conference, Cambridge, MA, USA, 12–15 September 2010.

15.　Rahman, M.A.; Anwar, S.; Izadian, A. Electrochemical Model Based Fault Diagnosis of Lithium Ion Battery. *Adv. Automob. Eng.* **2016**, *5*. [CrossRef]

16.　U.S. Department of Energy. PNGV Battery Test Manual, Rev. 0. July 1997. Available online: https://www.osti.gov/scitech/servlets/purl/578702 (accessed on 23 August 2017).

17.　Rahman, M.A.; Anwar, S.; Izadian, A. Electrochemical model parameter identification of a lithium-ion battery using particle swarm optimization method. *J. Power Sources* **2016**, *307*, 86–97. [CrossRef]

18. Stetzel, K.D.; Aldrich, L.L.; Trimboli, M.S.; Plett, G.L. Electrochemical state and internal variables estimation using a reduced-order physics-based model of a lithium-ion cell and an extended Kalman filter. *J. Power Sources* **2015**, *278*, 490–505. [CrossRef]

19. Lee, Y.-S.; Cheng, M.-W. Intelligent control battery equalization for series connected lithium-ion battery strings. *IEEE Trans. Ind. Electron.* **2005**, *52*, 1297–1307. [CrossRef]

20. Smith, K.A.; Rahn, C.D.; Wang, C.-Y. Control oriented 1D electrochemical model of lithium ion battery. *Energy Convers. Manag.* **2007**, *48*, 2565–2578. [CrossRef]

21. Chaturvedi, N.A.; Klein, R.; Christensen, J.; Ahmed, J.; Kojic, A. Algorithms for advanced battery-management systems. *IEEE Control Syst.* **2010**, *30*, 49–68. [CrossRef]

22. Klein, R.; Chaturvedi, N.A.; Christensen, J.; Ahmed, J.; Findeisen, R.; Kojic, A. State estimation of a reduced electrochemical model of a lithium-ion battery. In Proceedings of the American Control Conference (ACC), Baltimore, MD, USA, 30 June–2 July 2010.

23. Albertus, P.; Christensen, J.; Newman, J. Experiments on and modeling of positive electrodes with multiple active materials for lithium-ion batteries. *J. Electrochem. Soc.* **2009**, *156*, A606–A618. [CrossRef]

24. Subramanian, V.R.; Boovaragavan, V.; Ramadesigan, V.; Arabandi, M. Mathematical model reformulation for lithium-ion battery simulations: Galvanostatic boundary conditions. *J. Electrochem. Soc.* **2009**, *156*, A260–A271. [CrossRef]

25. Subramanian, V.R.; Diwakar, V.D.; Tapriyal, D. Efficient macro-micro scale coupled modeling of batteries. *J. Electrochem. Soc.* **2005**, *152*, A2002–A2008. [CrossRef]

26. Muddappa, V.K.; Anwar, S. Electrochemical model based fault diagnosis of li-ion battery using fuzzy logic. In Proceedings of the ASME 2014 International Mechanical Engineering Congress and Exposition, Montreal, QC, Canada, 14–20 November 2014.

27. Rahman, M.A. Electrochemical Model Based Fault Diagnosis of Lithium Ion Batteries. Master's Thesis, Purdue University, West Lafayette, IN, USA, 2015.

28. Speltino, C.; Domenico, D.D.; Fiengo, G.; Stefanopoulou, A. Experimental identification and validation of an electrochemical model of a lithium-ion battery. In Proceedings of the American Control Conference, Budapest, Hungary, 23–26 August 2009.

29. Eberhart, R.C.; Kennedy, J. A new optimizer using particle swarm theory. In Proceedings of the Sixth International Symposium on Micro Machine and Human Science, Nagoya, Japan, 4–6 October 1995.

30. Izadian, A.; Famouri, P. Fault diagnosis of MEMS lateral comb resonators using multiple-model adaptive estimators. *IEEE Trans. Control Syst. Technol.* **2010**, *18*, 1233–1240. [CrossRef]

31. Izadian, A.; Khayyer, P.; Famouri, P. Fault diagnosis of time-varying parameter systems with application in MEMS LCRs. *IEEE Trans. Ind. Electron.* **2009**, *56*, 973–978. [CrossRef]

32. Hanlon, P.D.; Maybeck, P.S. Multiple-model adaptive estimation using a residual correlation Kalman filter bank. *IEEE Trans. Aerosp. Electron. Syst.* **2000**, *36*, 393–406. [CrossRef]

33. Eide, P.K. Implementation and Demonstration of a Multiple Model Adaptive Estimation Failure Detection System for the F-16. Master's Thesis, Air University, Montgomery, AL, USA, 1994.

34. Eide, P.; Maybeck, P. An MMAE failure detection system for the F-16. *IEEE Trans. Aerosp. Electron. Syst.* **1996**, *32*, 1125–1136. [CrossRef]

35. Rahman, M.A.; Anwar, S.; Izadian, A. Electrochemical model based fault diagnosis of a lithium ion battery using multiple model adaptive estimation approach. In Proceedings of the 2015 IEEE International Conference on Industrial Technology (ICIT), Seville, Spain, 17–19 March 2015.

36. Eide, P.; Maybeck, P. Implementation and demonstration of a multiple model adaptive estimation failure detection system for the F-16. In Proceedings of the 34th IEEE Conference on Decision and Control, New Orleans, LA, USA, 13–15 December 1995.

37. Hunt, G.; Motloch, C. *Freedom Car Battery Test Manual for Power-Assist Hybrid Electric Vehicles*; INEEL: Idaho Falls, ID, USA, 2003.